Journal of Applied Science and Environmental Studies
JASES
http://revues.imist.ma/index.php?journal=jases

Original Paper

FP-LAPW STUDY OF STRUCTURAL, ELECTRONIC AND OPTICAL PROPERTIES OF TERNARY HgxCd1-xTe FOR OPTOELECTRONIC APPLICATIONS

F. BELARBIA [(a)] , Y. CHERCHEB[(a,b)], N. BELOUFA [(b)*], S. FASLA[(b)], D. SLAMNIA[(c)]

[(a)]University Relizane , Laboratory of Exact Sciences, BP 48000, Bormadia, 048000 Relizane, Algeria
[(b)]Laboratory of Micro and Nanophysics (LaMiN), National Polytechnic School Oran, ENPO-MA, BP 1523, El M'Naouer, 31000, Oran, Algeria
[(c)]ECP3M Abdelhamid Ibn Badis University Mostagenem Algeria

* Corresponding author. E-mail address: beloufa.nabil@gmail.com

Received 01February 2021; Revised 04 June 2021, Accepted 24 August 2021

Keywords
HgCdTe, GGA,
TB – mBJ, DFT.

Abstract

Despite its limitations (high cost, fragility, etc.), the HgCdTe ternary has qualities for infrared applications that are often superior to those of its competitors. One main purposes of the present work is to review the known data of this material, to list its advantages but also its disadvantages. As exchange–correlation potential we used the generalized gradient approximation (GGA) of Perdew et al. in addition the modified Beck-Johnson potential (TB – mBJ) approach, and implemented in the WIEN2k calculation code. The band gap energy values of materials have been improved by the use of the recent approximation of (TB – mBJ) where the results are very close with the experimental data. The results obtained have been compared with experimental data from the literature and other results of theoretical work.

1. Introduction

In particular, there has been a growing demand for quantitative imaging and spectrometry, such as multi- and hyperspectral imaging based on the use of matrix detectors called focal plane IR (PFIR) detectors (1) -(3) These devices allow the

extraction of spatial (imaging), spectral (spectrometry), or simultaneous spatial and spectral (spectro-imaging) information from the image of a scene (4).Among the many applications targeted are gas detection in the industrial context (5),high rate spectra restitution (6),night vision (7),surveillance (8),and ballistic missile defence systems (9).Faced with such needs, the systems developed have increasing requirements in terms of profitability, performance, consumption, compactness and weight (10).

The CdTe and HgTe binary belong to the II-VI semiconductors crystallize in the Zinc-blende phase which is their equilibrium phase. The ternary $Hg_xCd_{1-x}Te$ for (x= 0.25, x=0.5, x=0.75) using the wien2k code based on the DFT theory. We have constructed $Hg_xCd_{1-x}Te$ in this work from the zinc-blende phase atomic positions of HgTe but by replacing some Hg atoms by Cd atoms. The number of atoms replaced depends on the desired stoichiometry. The symmetry of the ternary HgCdTe is not Zinc-Blende but rather the conventional single cubic mesh which is a larger cell and also because the arrangement of the atoms changes the previous symmetry.

Mercury cadmium telluride (HgCdTe), often called mercatel (MCT), is an alloy of mercury telluride (HgTe) and cadmium telluride (CdTe). There is a good mesh agreement between CdTe and HgTe, which makes it possible to obtain very good quality epitaxial hetero structures. HgCdTe is a semiconductor ternary alloy discovered in 1959 and is also the 3rd most important semiconductor after silicon and gallium arsenide. It shows superior performance in most infrared (IR) applications: SWIR Detection and Imaging (1-3µm), MWIR (3-5µm), LWIR (8-14µm), VWIR (14-30µm). It allows to obtain focal plane arrays for practical applications ranging from night vision, to surveillance and reconnaissance.

2. Computational details

First we calculated the variation in total energy as a function of volume and then used the Murnaghan equation (11), to obtain the equilibrium mesh parameter a_0, as well as the modulus of compressibility and its derivative with respect to pressure. Then, using the exchange potential of Perdew et al (12) ,and me potential mBJ (14), implemented in the FP-ALPW method we calculated the band structures, the densities of states (DOS: Density Of States which represent the number of electronic states per unit of energy), the charge densities and the optical properties.

In this work, semi-relativistic calculations were performed. Wave functions, electron densities and potential are developed in spherical harmonic combinations around atomic sites, in the spheres Muffin-tin with a cut-off (cut-off radius), and in Fourier

series in the interstitial region with a cut-off (cut-off radius) Rmt ∗Kmax (where Rmt is the smallest radius of the MT sphere, Kmax is the cut-off of the wave vector for plane waves) we used the value Rmt ∗Kmax =8 and lmax = 10. The first step in such calculations is to specify the values of important parameters, which affect the time and accuracy of the calculation.

The Muffin-tin radii (Rmt) are given in atomic units (a.u). The values from Rmt_{min} that we used for Cd (2.5), Hg (2.5), Te(2.4), are a good choice for our calculation. This choice is based on two criteria:

- Make sure that the majority of the core electrons are integrated in the sphere (Muffin-tin).
- Avoid overlapping spheres (Muffin-tin).

The cut-off parameter RKmax = Rmt ∗Kmax , with Rmt is the smallest radius of the sphere MT and Kmax is the norm of the largest wave vector used for plane wave development of eigen functions. Gmax is the norm of the largest wave vector used for plane wave development of the eigen functions.

The number of k-points considered in the Brillouin irreducible zone. However, all the results represented are obtained with a convergence of the order of 0.5mRyd. Strip structures for our materials are calculated according to different points of high symmetry: for (111) points in the Brillouin zone.

Thus the II-VI bond results from the sp3 hybridization of the atomic orbitals, this bond is iono-covalent with an ionicity character which provides the II-VI semiconductors with a remarkable property: strong Coulombic interactions, whereas the covalent character imposes the following structure on them: each element II (respectively element VI) is found in a tetrahedral environment of element VI (respectively element II).

II: a cation, also called a transition metal, having two valence electrons on an "s" orbital, as well as a "d" layer which can be either complete or incomplete.

VI: An anion with six valence electrons.

In our calculations, we have treated the states: The Cd states: ($4d^{10}$ $4s^2$), Hg: ($5d^6$ $6s^2$), Te ($5s^2$ $5p^4$) as valence states. we note that the convergence criteria are verified (Rmt*kmax, Kpoint and lmax).

3. Structural properties

We took a conventional cubic HgCdTe cell containing eight atoms, of which four atoms of Cd and four other atoms of Te. In this model, the alloy has simple cubic

symmetry. In the eight-atom model, the alloy $Hg_{0.25}Cd_{0.75}Te$ is obtained by replacing one atom of Hg with atom of Cd. The $Hg_{0.5}Cd_{0.5}Te$ is obtained by replacing two Hg atoms with two Cd atoms and finally for the $Hg_{0.25}Cd_{0.75}Te$ it is sufficient to replace three Hg atoms with three further Cd atoms.

Figure 1 shows the variation of the total energy of *HgCdTe* in single cubic phase with volume in the three cases of alloy. After fitting using Murnaghan's equation of states (11),we note that for total equilibrium energy, the corresponding equilibrium volume is V_0= 1986.1081 $(u.a)^3$, 1978.8674 $(u.a)^3$, and 1973.362$(u.a)^3$ for x = 0.25, 0.5 and 0.75, respectively. This implies that the network constants are 12.57 a.u ,12.55 a.u and 12.54 a.u, respectively. The bulk modulus coefficient of compressibility found is B= 34.75 GPa, 35.44GPa and 34.52 GPa.

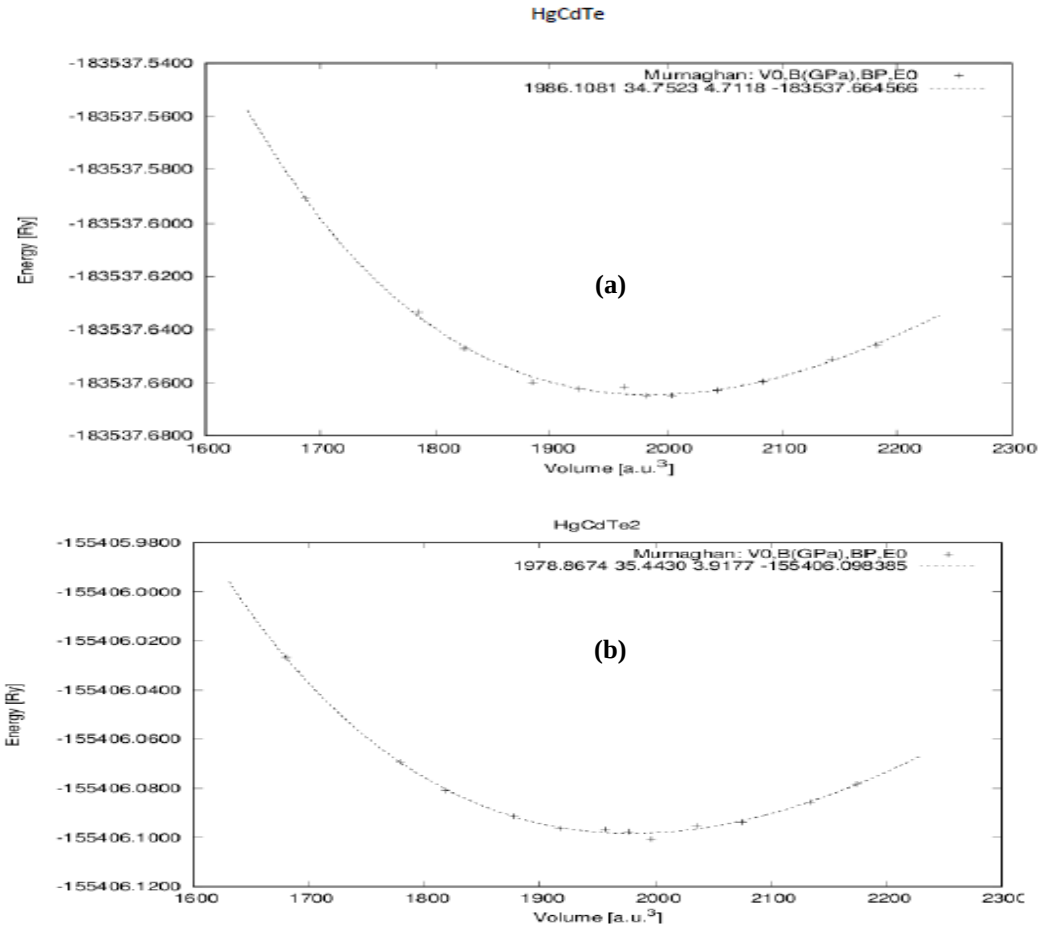

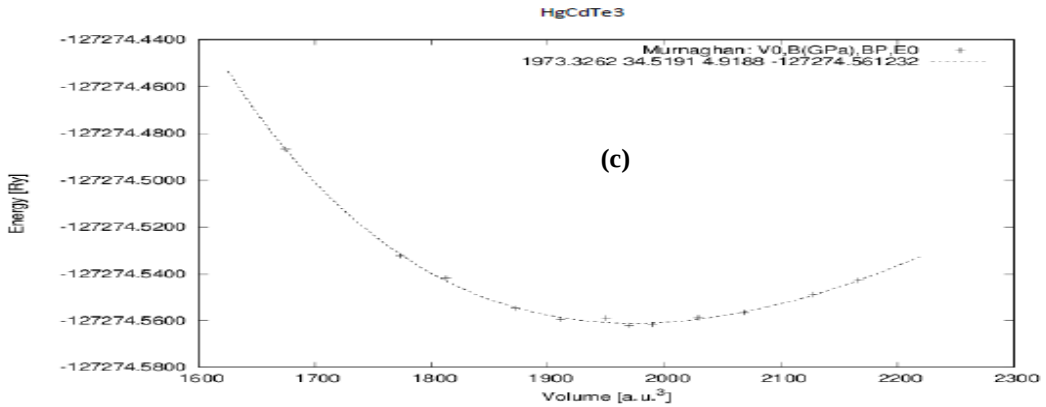

Fig 1. Total Energy (eV) as a function of the volume (a.u^3) for $Hg_xCd_{1-x}Te$ at concentrations (a) x = 0.25, (b) x = 0.50 and (c) x = 0.75.

	Our Work			**Other Work**
	$Hg_{0.25}Cd_{0.75}Te$	$Hg_{0.5}Cd_{0.5}Te$	$Hg_{0.75}Cd_{0.25}Te$	
Volume	1973.3262	1978.8674	1986.1081	1843.24[a]; 1867.68[a] ; 1867.68[a]
a_0**(Å)**	6.635	6.64	6.65	6.49[a] ; 6.52[a] ; 6.51[a]
B(GPa)	34.52	35.44	34.75	44.574[a] ; 42.367[a] ; 43.250[a]
E_0**(eV)**	-127274.561	-155406.09	-183537.664	/

Table 1. Calculated lattice parameter (a_0), Volume(V_0),energy(E_0), and bulk modulus (B) for $Hg_xCd_{1-x}Te$ alloys.

[a] Reference (14).

The Variations in the lattice parameter of the alloy as a function of concentration x compared with those obtained with Vegard's law enforcement (15),are presented.by (Figure 2), where a decrease in lattice parameter as a function of the change in concentration. Vegard's law which is written as follows:

$$a_{(HgxCd1-xTe)} = x\, a_{HgTe} + (1-x)a_{CdTe} \qquad \text{Eq1}$$

where a_{HgTe} and a_{CdTe} are the equilibrium lattice constants of the binary compounds and the term $a_{(HgxCd1-xTe)}$ is the lattice constant of the ternary compound. we see a remarkable shift between the calculated network parameter curve and the following one Vegard's law, this implies the existence of a Bowing (adjustment) parameter important mainly due to: structural relaxation, crystal deformation and the difference in ionicity between the massifs (CdTe and HgTe) which translates into a transfer of load.

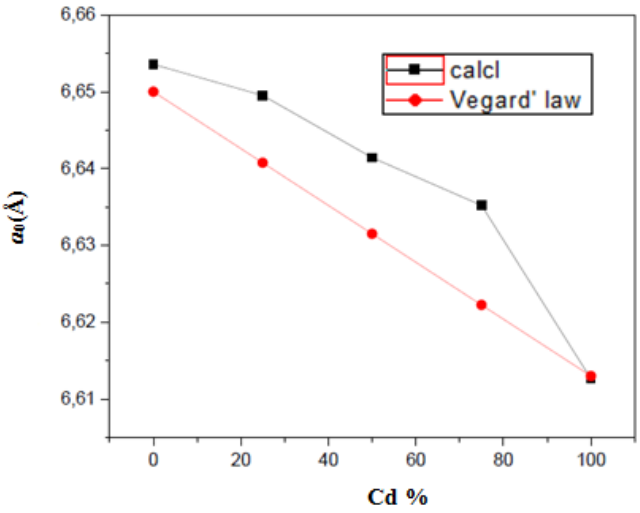

Fig.2 Composition dependence of the calculated lattice constant of $Hg_{1-x}Cd_xTe$ ternary alloys compared with Vegard' law.

4. Electronic properties

4.1 Band structure

The structures of the bands of $Hg_{0.75}Cd_{0.25}Te$, $Hg_{0.5}Cd_{0.5}Te$ and $Hg_{0.25}Cd_{0.75}Te$ are shown in (Figure 3).

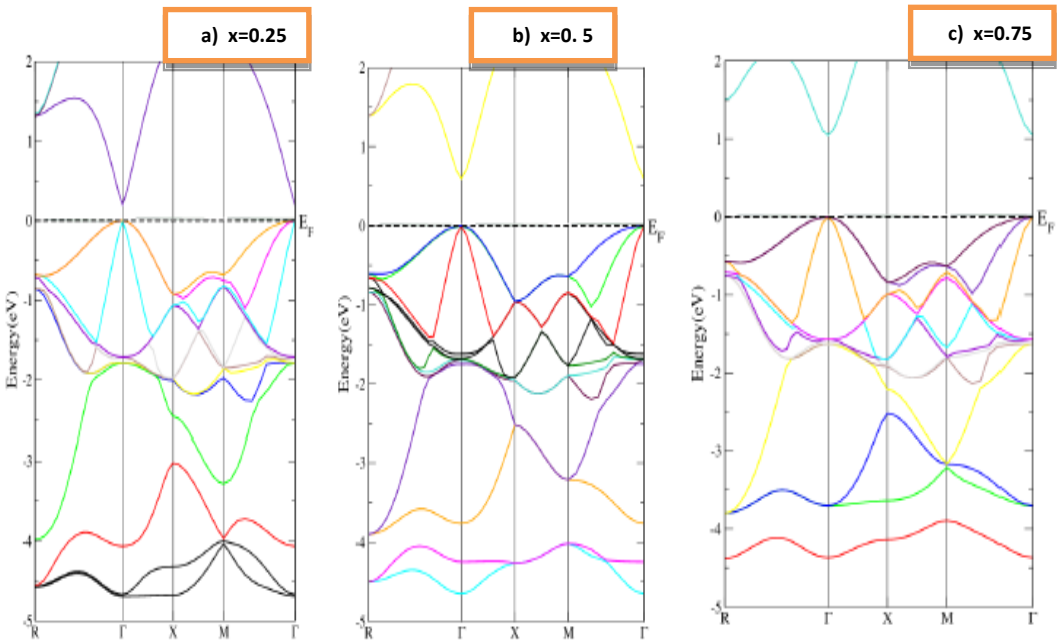

Fig. 3 Energy band structures for $Hg_xCd_{1-x}Te$ for concentrations of (a) x = 0.25, (b) x = 0.5 and (c) x = 0.5.

In the three cases of alloy, it can be seen that the minimum of the conduction band (BC) and the maximum of the valence band (BV) are located at the point □ , this direct gap is : 0.21 eV for x=0.25, and 0.62 eV for x=0.5 and 1.05 for x=0.75. These values are calculated with mbj.

Energy Gap (eV)	Our results (mBJ)		
	$Hg_{0.75}Cd_{0.25}Te$	$Hg_{0.5}Cd_{0.5}Te$	$Hg_{0.25}Cd_{0.75}Te$
(Γ→Γ)	0.21	0.62	1.05
(Γ →R)	1.31	1.39	1.51

Table.2 Gap energy Eg of $Hg_xCd_{1-x}Te$ ternary alloys.

In (Figure 4), we show the dependency of the band structure $Hg_xCd_{1-x}Te$ alloy according to composition x at Γ. Indeed, in the approximation of the virtual crystal VCA, the negative band gap for the HgTe structure, increases linearly with the composition x, until it reaches the structure of CdTe.

-HgCdTe shows a null gap when ($E_{\Gamma 8}$)- ($E_{\Gamma 6}$)= 0 for x=x ≈16%.

-For x <x, the alloy has the same semi-metallic structure as HgTe.

-For x >x, the state Γ_6 is above the state Γ_8, and at the same time the band Γ_6 and Γ_8 change sign as the gap opens.

In our work, the variation of the $Hg_xCd_{1-x}Te$ gap as a function of the composition x is reported in (Figure 4). We have applied the VCA (the approximation of the crystal virtual) (16), which gives the gap of the alloy as a function of the concentration x.

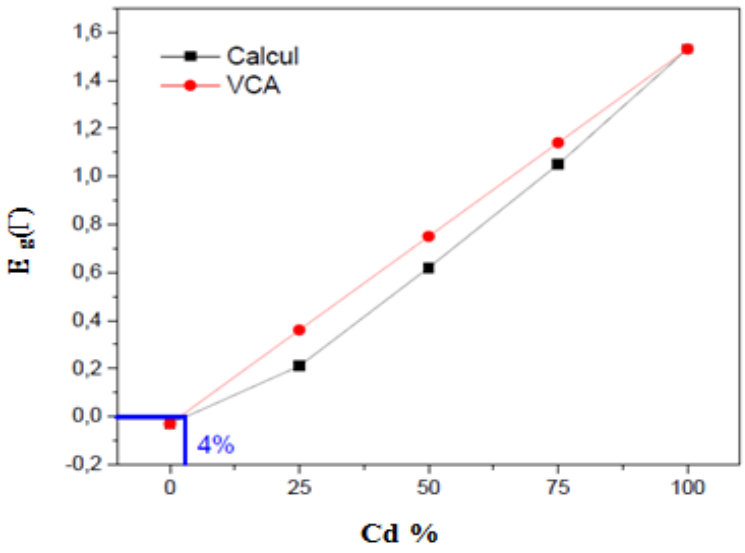

Fig. 4 Gap variation of $Hg_{1-x}Cd_xTe$ alloy as a function of composition x in Cd %.

As can be seen in (Figure 4), this variation of the gap of $Hg_xCd_{1-x}Te$ is increasing in Cadmium concentration "Cd" at room temperature and ranges from -0.03 in HgTe to +1.53eV in CdTe. x =4% is the critical value of the concentration for which it is measured. produces the semi-metal-semiconductor transition with Eg = 0.

This variation of the gap $Hg_xCd_{1-x}Te$ is in very good agreement with the results experimental (17).

4.2 Density of charge

The description of the charge density is an important property in solids, since it provides a good description of the chemical properties. The ionic character is related to the charge transfer between cations and anions. For this reason we have calculated the Density of charge of the alloy $Hg_xCd_{1-x}Te$ in the different concentrations using the GGA approximation, the results of the load density are shown on the figures (Figure 5.a-5.c).we have chosen the plane (110). We say we have a ionic character when the charge is concentrated around the atomic spheres of the atoms, while it is absent in the interstitial regions. When the interstitial spaces are full, we have a dominant covalent character. The element Te (2.1) has a slightly larger electronegativity than that of element Cd(1.7) and Hg(1.9) so we notice an electronic site load transfer cationic to anionic site.

a) $Hg_{0.25}Cd_{0.75}Te$ b) $Hg_{0.5}Cd_{0.5}Te$ c) $Hg_{0.75}Cd_{0.25}Te$

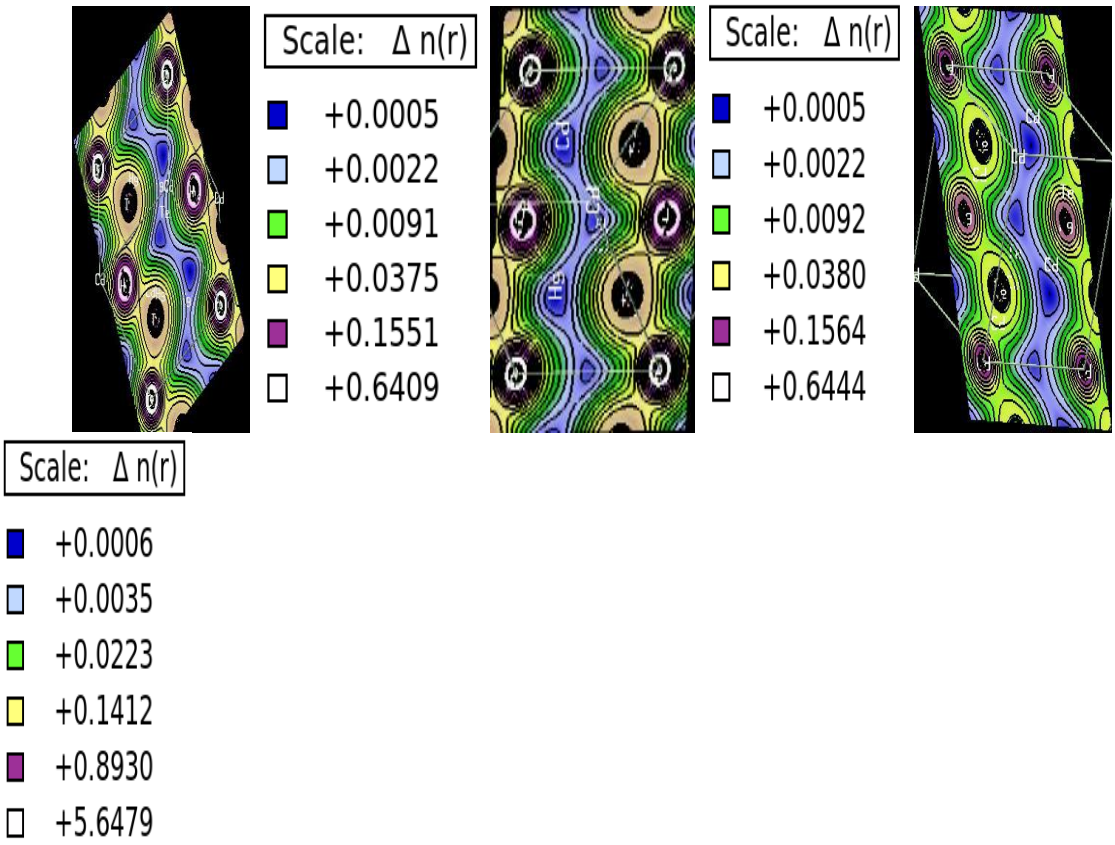

Fig. 5 The density of charge of: a) $Hg_{0.25}Cd_{0.75}Te$, b) $Hg_{0.5}Cd_{0.5}Te$ and c) $Hg_{0.75}Cd_{0.25}Te$**.**

The Table 2 include charge transfer values in the cationic sires, the anion site and theinterstitial region

Table. 3 The different charge transfers in the alloy $Hg_xCd_{1-x}Te$.

Transfer of charge	**Our results**		
	$Hg_{0.75}Cd_{0.25}Te$	$Hg_{0.5}Cd_{0.5}Te$	$Hg_{0.25}Cd_{0.75}Te$
ΔQ^{Cd}	-0.244	-0.246	-0.248
ΔQ^{Hg}	-0.223	-0.226	-0.231
ΔQ^{Te}	0.036	0.051	0.068
$\Delta Q^{interstitial}$	0.7633	0.7326	0.6989

The (Figure 6) shows the variation in load density as a function of the cadmium concentration, there is a linear variation in the transfer of charge where the increase in charge transfer around the anion sites (Te) and the region interstitial, accompanied by deflection into cationic sites. It is concluded that there is the contribution of both ionic

and covalent characters in our $Hg_xCd_{1-x}Te$ alloy, such as the slight increase in ionicity from HgTe to the CdTe structure and accompanied by a decrease in covalency.

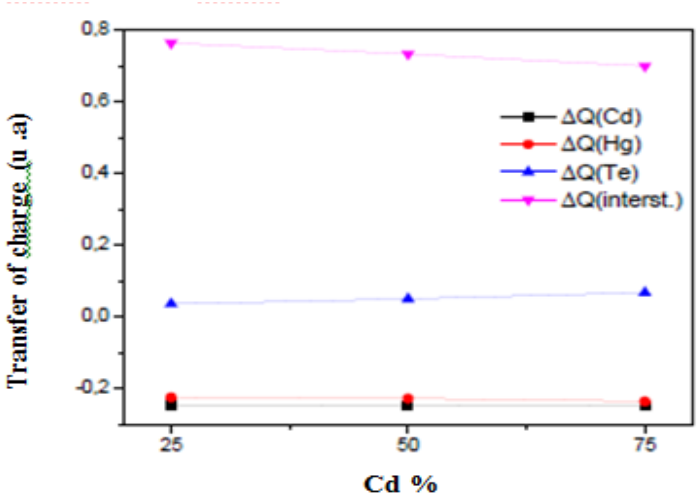

Fig. 6 Transfer of charge as a function of Cd%.

5. Optical properties

We present the variation of the constant static dielectric ε_{st} at zero frequency according to the composition in Cadmium (Cd) concentration in (Figure 7). For comparison, we have used the following empirical formula (17):

$$\varepsilon_s = 20.6\text{-}15.6x+5.7x^2 \qquad \text{Eq2}$$

It can be seen that the static dielectric constant ε_s decreases when the concentration of cadmium increases.

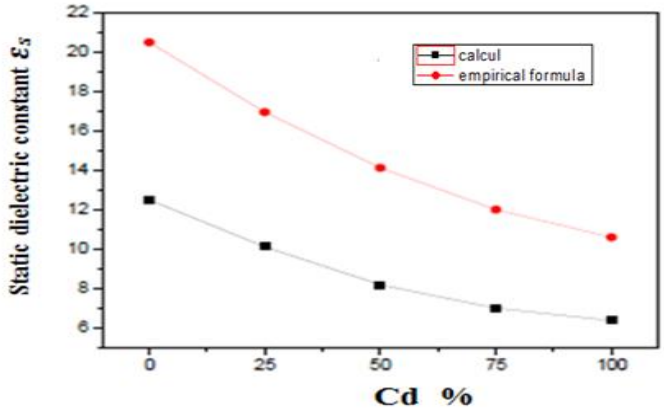

Fig. 7 Variation of the static dielectric constant of the alloy $Hg_xCd_{1-x}Te$ depending on the composition of Cd **.**

The absorption coefficient $\alpha(\omega)$ characterizes the part of energy absorbed by the solid, it can be defined as a function of the extinction coefficient by the relation :

$$\alpha(\omega) = \frac{4\pi}{\lambda} k(\omega) \qquad \text{Eq 3}$$

Where λ is the wavelength of light in vacuum. The absorption coefficient of $Hg_xCd_{1-x}Te$ is represented in (Figure 8) as a function of of the wavelength.

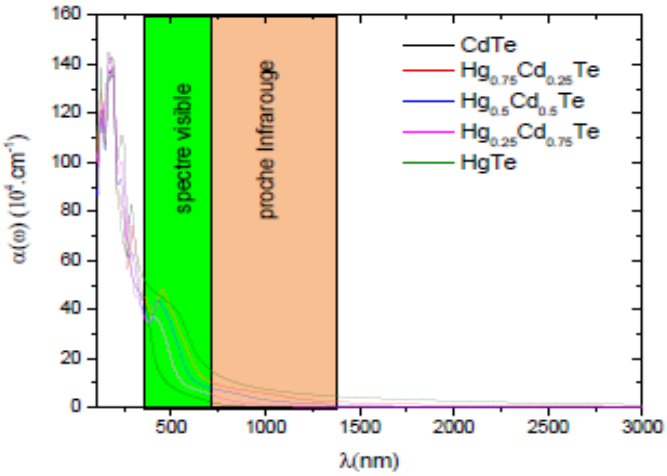

Fig. 8 The variation of the absorption coefficient as a function of wavelength.

For our materials the absorption coefficient increases with the energy of the incident wave. The intensity of the incident wave is related to the absorption coefficient in neglecting the loss of energy due to reflection by the following expression:

$$I(x) = I_0\, e^{-\alpha\, \omega\, (x)} \qquad \text{Eq4}$$

X: the thickness of the solid.

I_0: the intensity of the wave in vacuum.

By examining the absorption coefficient curves, it can be seen that the coefficient absorption begins to increase to a certain energy value beyond the length of the wave (corresponding to the excitation energy), the energy is no longer sufficient for extracting electrons, hence the sharp drop in absorption. We confirm that $Hg_xCd_{1-x}Te$ is characterized by low absorption in the near-infrared region relative to the visible region or the ultraviolet region.

We note that for $Hg_xCd_{1-x}Te$, where we have fundamental gap to a direct transition, the absorption coefficient is proportional to $(h\nu - E_g)^{1/2}$

(Figure 9) shows the variation of the optical absorption coefficient in the alloy $Hg_xCd_{1-x}Te$, this coefficient starts to increase very quickly as soon as the energy of gap E_{g0}.

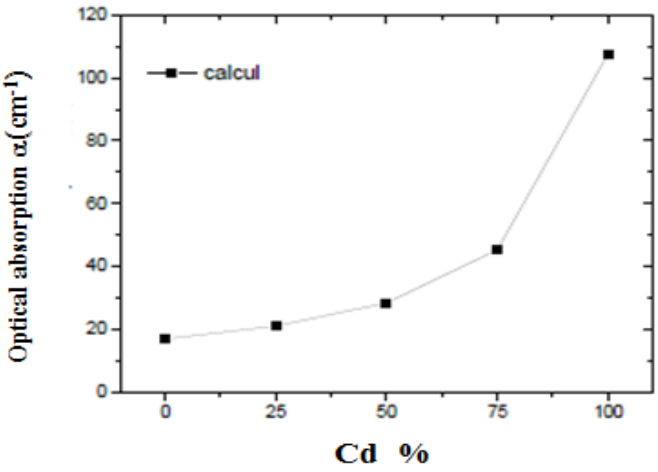

Fig. 9 The variation of the optical absorption coefficient in the alloy $Hg_x Cd_{1-x}Te$.

The reflectivity of light is important in the calculation of optical properties; indeed, reflectivity is sensitive to the complicated combination of the function dielectric. We illustrate on (Figure 10), the reflectivity for deferents concentrations of 0%, 25%, 50%, 75% and 100%, we present a comparison between the reflectivity curves as a function of wavelength. All concentrations have reflectivities of approximately 30%. *$Hg_xCd_{1-x}Te$* is found to have oscillations in reflectivity that increase up to the visible region and then they decrease in the near-infrared region (NIR region). The CdTe is significantly lower than the HgTe reflectivity. It is also noted that the reflectivity for all three concentrations continues to decrease in the infrared region.

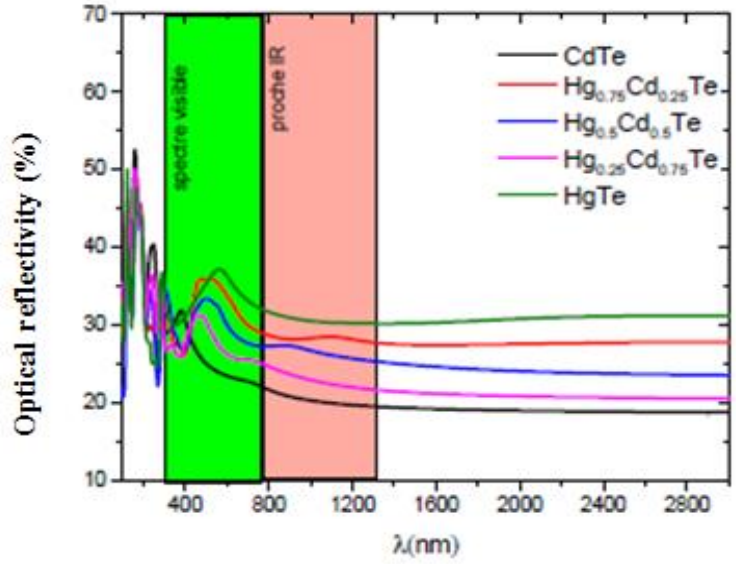

Fig. 10 Comparison of the optical reflectivity as a function of length waveform (□) of $Hg_x Cd_{1-x}Te$.

The (Figure 11), illustrates the curve of the optical transmittance of deferents Cadmium concentrations. It can be seen that the curves are characterized by a high transmittance

in the near and mid-infrared regions (NIR and MIR) and low values in the Ultraviolet (UV) and visible region. Transmittance is the theoretical formulas are combined

$$T = (1 - R)^2.e^{-\alpha d} \qquad \text{Eq5}$$

Where

$$T + A + R = 1 \qquad \text{Eq6}$$

Such as:

T: represents optical transmittance.

R: represents optical reflectivity.

and

A: represents absorbance where it is related to absorption by the following relationship:

$$A = e^{-\alpha d} \qquad \text{Eq7}$$

The transmittance of pure CdTe is about 66% in the MIR. Indeed, the reflectivity makes reduce the ideal value (100%) by about 30% in the NIR region. We can also see that $Hg_{1-x}Cd_xTe$ alloy has low transmittance values in the region of ultraviolet (UV) and visible light

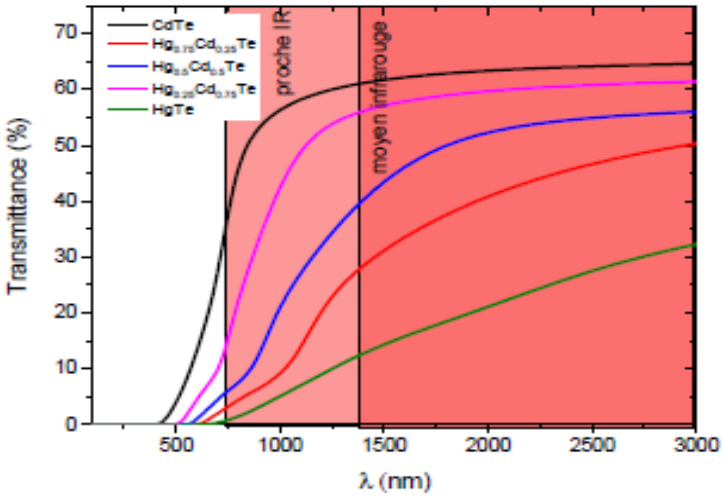

Fig. 11 Comparison of the Optical Transmittance vs. wavelength (λ) in (nm) of $Hg_x Cd_{1-x}Te$.

Conclusion

In this work, we were interested in the study of structural properties, electronic and optical ternary HgCdTe . This alloy is a major player in the field of infrared in general and imaging and night vision in particular, using the linear plane wave method (FP-LAPW) within the framework of the Density Functional Theory (DFT) implemented in

the WIEN2k code. We used the generalized gradient approximation GGA, and to perform the gap calculation we used the mBj approximation. The results obtained can be summarized as follows:

On sees a network parameter decrease as a function of the variation of the on concentration Cd%. There is a remarkable shift between the network parameter curve calculated and according to Vegard's law, this implies the existence of a Bowing parameter mainly due to: relaxation of the structure, deformation of the crystal and the difference in ionicity between the masses (CdTe and HgTe) which translates into a load transfer.

Band structure: In the three cases of alloy, we can see that the minimum of the strip conduction (BC) and the maximum of the valence band (BV) are located at the point Γ , this gap direct is: 0.21 eV for x=0.25, and 0.62 eV for x=0.5 and 1.05 for x=0.75. These values are calculated with mbj, this variation of the gap of $Hg_xCd_{1-x}Te$ .Te is increasing in concentration of Cadmium "Cd" at room temperature and ranges from -0.03 in HgTe) to +1.53eV in CdTe. x =4% is the critical concentration value for which it is the most important. Produces the semi-metal-semiconductor transition with Eg = 0.

On notes that there is a linear variation in load transfer where the increase in the charge transfer around the anionic sites (Te) and the interstitial region, accompanied by with a deflection in the cationic sites. We conclude that there is the contribution of both ionic and covalent characteristics in our $Hgx Cd1-x Te$ alloy, such as the increase in of the ionic character from HgTe to CdTe structure and accompanied by an decreased covalency.

It is concluded that the length of the link decreases slightly with the increase in the cadmium concentration, where the change in bond length from 0% to 100% is only 0.9%. We note that the link length is very higher than hard materials (diamond, graphite, etc.) which are of the order of 2.64 u.a (1.4 Å) (very short), from which it is concluded that the bonds in the HgCdTe ternary are which are sensitive to crystal growth.

We have studied the optical properties, where we have concluded that:

-We find that the static dielectric constant decreases when the concentration of cadmium increases.

- $Hg_xCd_{1-x}Te$ is confirmed to be characterized by low absorption in the region near-infrared to the visible or ultraviolet region.

-We note that for $Hg_xCd_{1-x}Te$, of direct fundamental gap, the coefficient of absorption is proportional to $(h\nu - E_g)^{1/2}$. The optical absorption coefficient in the $Hg_xCd_{1-x}Te$ alloy starts to increase very rapidly as soon as the gap energy Eg_0.

- $Hg_xCd_{1-x}Te$ is found to exhibit reflectivity oscillations that increases up to the visible region and then decreases in the near region.

infrared (NIR region).-Reflectivity for all three concentrations continues to decrease in all three regions

- The infrared region, the curves are characterized by high transmittance in the near and mid-infrared regions (NIR and MIR) and low values in the region Ultraviolet (UV) and the visible region.

References

1. P. Dixon, C.D. Hess, C. Li, M. Ettenberg et J. Trezza, **International Society for Optics and Photonics**, (2011).80121V–80121V.

2. Y. Reibel, F. Chabuel, C. Vaz, D. Billon-Lanfrey, J. Baylet, O. Gravrand, P. Ballet and G. Destefanis, .**International Society for Optics and Photonics**, (2011). 801238–801238

3. T. Skauli, H.E. Torkildsen, I. Kåsen, S. Nicolas, T.V. Haavardsholm and T.O. Opsahl, **Optical Society of America**, 2013.

4. Y. Ferrec, « Spectro-imageur », Tech. Ing., **Mesures et contrôle**, (2007). (e4111).

5. V. Farley, A. Vallieres, A. Villemaire, M. Chamberland, P. Lagueux and J. Giroux,. **International Society for Optics and Photonics**, (2007). 673918–673918

6. N. Guerineau, S. Suffis, P. Cymbalista and J. Primot, **International Society for Optics and Photonics**, (2004) 441–448

7. H. Lutz, R. Breiter, S. Rutzinger, T. Schallenberg, J. Wendler and J. Ziegler, **International Society for Optics and Photonics**, (2013) 87040A–87040A.

8. T. Martin, R. Brubaker, P. Dixon, M-A. Gagliardi and T. Sudol, **In SPIE Defense and Security**, (2005). 13.

9. M.Z. Tidrow, "New infrared sensors for ballistic missile defense", **International Society for Optics and Photonics**, (2005). 217–224.

10. P. Norton, **Opto-Electron**. (2006) Rev 14, 1.

11. P. Hohenberg, W. Kohn, **Phys. Rev** (1964) 136, B864

12. W. Kohn, L.S. Sham, **Phys. Rev** (1965) 140, A1133

13. F.D. Murnaghan, **Proc. Natl. Acad. Sci**. (1944). 30, 5390

14. A. Rogalski, P. Martyniuk, and M. Kopytko, **Appl. Phys .Rev**. (2017)..4,031304

15. Vegard: L. Vegard, Z. **Phys** (1921) . 5 17.

16. J.R. Lowney, D.G. Seiler, C.L. Littler, and I.T. Yoon, **J. Appl. Phys** (1992) .71,1253

17. Rogalski, Prog**. Phys (**2005) .68. 2267-2336.

.